

PCCP

Accepted Manuscript



This article can be cited before page numbers have been issued, to do this please use: J. Martinez-Asencio, C. Ruestes, E. M. Bringa and M. J. Caturla, *Phys. Chem. Chem. Phys.*, 2016, DOI: 10.1039/C6CP01487A.



This is an *Accepted Manuscript*, which has been through the Royal Society of Chemistry peer review process and has been accepted for publication.

Accepted Manuscripts are published online shortly after acceptance, before technical editing, formatting and proof reading. Using this free service, authors can make their results available to the community, in citable form, before we publish the edited article. We will replace this *Accepted Manuscript* with the edited and formatted *Advance Article* as soon as it is available.

You can find more information about *Accepted Manuscripts* in the [Information for Authors](#).

Please note that technical editing may introduce minor changes to the text and/or graphics, which may alter content. The journal's standard [Terms & Conditions](#) and the [Ethical guidelines](#) still apply. In no event shall the Royal Society of Chemistry be held responsible for any errors or omissions in this *Accepted Manuscript* or any consequences arising from the use of any information it contains.

How controlled rippling of graphene via irradiation and applied strain can modify its mechanical properties: a nanoindentation simulation study*

J. Martinez-Asencio[†], C. J. Ruestes[‡], E. M. Bringa, M. J. Caturla[†]

ABSTRACT

Ripples, present in free standing graphene, have an important influence in the mechanical behavior of this two-dimensional material. In this work we show through nanoindentation simulations, how out-of-plane displacements can be modified by strain resulting in softening of the membrane under compression and stiffening under tension. Irradiation also induces changes in the mechanical properties of graphene. Interestingly, compressed samples, irradiated at low doses are stiffened by the irradiation while samples under tensile strain do not show significant changes in their mechanical properties. These simulations indicate that vacancies, produced by the energetic ions, cannot be the ones directly responsible for this behavior. However, changes in roughness induced by the momentum transferred from the energetic ions to the membrane, can explain these differences. These results provide an alternative explanation to recent experimental observations of stiffening of graphene under low dose irradiation, as well as paths to tailor the mechanical properties of this material via applied strain and irradiation.

INTRODUCTION

Graphene is a single layer of graphite, an atom thick allotrope of carbon arranged in a honeycomb lattice which presents a sp² hybridization. This singular stable structure presents some unique physical properties, such as excellent electronic transport^{1,2}, thermal conductivity^{3,4}, optical^{5,6} and mechanical response⁷ especially for its elasticity and intrinsic strength features. All these make graphene one of the most promising and attractive materials of recent years. Therefore, it is being studied for a vast variety of applications. For instance, transistors⁸⁻¹⁰, transparent electronic materials¹¹ and sensors in nanoelectronics¹², cancer therapy¹³ in medicine, solar cells¹⁴ in energy storage industry and even conducting ink^{15, 16} manufacturing, are some of many possible uses of this promising material.

One method of altering¹⁷ the above mentioned physical and chemical properties, and possibly enhancing them, consists of studying a graphene layer with impurities or defects, like adatoms, dislocations or vacancies. There are many ways to produce defects on a sample^{18, 19}, but a simple and efficient way to create them in a controlled manner is by ion bombardment. For these methods to be efficient and feasible it is important to understand the type of defects produced under the different irradiation conditions, such as irradiation type (electrons or ions), temperature, energy and dose. Tuning energy and dose can lead to formation of nanopores²⁰.

* Electronic supplementary information (ESI) available

[†] Dept. Física Aplicada, Facultad de Ciencias, Fase II, Universidad de Alicante, Alicante E-03690, Spain, e-mail: mj.caturla@ua.es

[‡] CONICET and Facultad de Ciencias Exactas y Naturales, Universidad Nacional de Cuyo, Mendoza 5500 Argentina

²¹, and some stable structures such as monoatomic chains²². Damage produced by irradiation in supported graphene as well as multilayer graphene has also been studied by several authors both experimentally and computationally (see for example ref. 23-26).

Numerous studies of irradiation damage have been performed using molecular dynamics for electron²⁷ or ion implantation²⁸⁻³². Irradiation of graphene with C ions, ranging from 0.1 eV to 100 keV at different positions on the hexagonal lattice has been studied by Bellido and Seminario²⁹ and a similar study was carried out with Si ions³⁰. An experiment combined with MD simulations using Ar⁺ ions on graphene/Ir(111) was performed for different beam energies³³. Also, an experimental study based on Ar⁺ bombarded graphene on a SiO₂ substrate has been performed by Dobrik et al.³⁴, where they concluded that the Fermi velocity is reduced in the presence of defects. Increasing the quantity of defects in graphene leads to weakening of its robustness, making it less stiff and degrading its mechanical properties^{35, 36}. More recent experiments³⁷, however, have shown that irradiation of suspended graphene using low energy Ar ions give rise to increased stiffness of the graphene membrane when defect concentrations are around 0.1-0.2%, reporting values of two-dimensional Young modulus (E_{2D}) higher than for pristine graphene⁷. Several explanations have been proposed for the mechanism of stiffening of graphene at such low defect concentration^{37, 38}.

One important phenomenon in two-dimensional systems such as graphene that might have been overlooked is the influence of the out-of-plane displacements present in these structures. It is well-known that graphene is not perfectly flat, but it forms ripples^{39, 40} which appear due to thermal fluctuations and its two-dimensional nature. The structure of these ripples and their influence in different properties of graphene, including elastic properties⁴¹, has been the interest of many studies⁴²⁻⁴⁴. Recent molecular dynamics simulations have shown that intrinsic ripples of graphene affect its elasticity, resulting in softening of this material⁴¹.

In this paper we present molecular dynamics simulations of the irradiation of suspended graphene membranes with 140 eV Ar ions for different values of the initial strain at 300K. We focus on the nature of those defects produced by the irradiation as a function of dose and applied strain, as well as the changes in the ripple distribution and roughness. Nanoindentation simulations of the graphene membrane show how the mechanical properties of this material change for different conditions of applied strain and irradiation.

METHODS

Classical molecular dynamics (MD) simulations of irradiation have been performed using the LAMMPS code⁴⁵. A graphene drumhead of radius 75 nm which contained 674644 carbon atoms was used for these calculations. The Tersoff/ZBL potential was used to simulate the C-C interaction. This potential accounts for 3-body interactions using the Tersoff potential⁴⁶ and also short-range interactions between atoms mimicking a Coulombic repulsive potential using a screening function described by the so-called ZBL potential, Ziegler-Biersack-Littmarck⁴⁷ which is needed for the short distance interactions that occur when performing irradiation simulations. The ZBL potential was then used for the Ar-C and Ar-Ar interactions. The Tersoff potential has been used by other authors to study damage production in graphene^{21, 28, 29, 38, 48}.

Fixed boundary conditions were considered in the outer layer of the drumhead. The regions are set as follows: an outermost annulus of 1 nm with fixed atoms, an adjacent annulus of 2 nm with a Langevin thermal bath and a dynamical region for the rest of the drumhead. In this way, we achieve simulating a suspended graphene flake with a cooling down region, so that a smooth transition between the dynamic region and the one with fixed atoms takes place. The simulation

volume is relaxed using the Polak-Ribière version of the conjugate gradient algorithm⁴⁹ so that any residual stress is removed. Simulations were also performed for different initial strains, from compressive to tensile, with values between -0.25% and 0.25%, respectively. For those simulations where an initial strain is applied, the strain is produced by changing the simulation box size and remapping the atomic positions according to the new box size. Then, the system is relaxed for 3 ps in NPH ensemble at P=0 bars in the x and y axis and a temperature of 300K. The time step used in these simulations is 1 fs.

Simulation of irradiation of the graphene drumhead is set as follows. After the system is relaxed to the selected strain conditions, the sample is irradiated with one low energy Ar ion (140 eV) every 5000 time steps, and a total of 1000 ions were shot. In this case, a variable time step is considered to account for the short range interaction of the energetic atoms. The sample was irradiated perpendicularly within a circular region of a radius of 65 nm from its center with the irradiation point selected randomly within this region. The system is equilibrated for 35000 steps after the 1000 ion irradiation. We employed the NVE ensemble during the irradiation for the inner region of the drumhead. Simulations have been performed at 300K.

One of the parameters that we have analyzed is the roughness of the membranes and how it evolves during irradiation. The roughness is calculated as the average of the square of the distance in the z direction (perpendicular to the membrane) with respect to the initial position, z_0 , of all atoms in the membrane, $\langle(z-z_0)^2\rangle$.

Defects are identified using OVITO⁵⁰ and are classified as monovacancies, divacancies, and higher order vacancy clusters (more than two vacancies). A first nearest neighbor distance is considered to identify if vacancies belong to the same cluster.

A set of drumheads was selected for indentation simulations to assess the effect of strain and irradiation on their mechanical properties, namely, its elastic modulus. Indentation was performed using a spherical indenter tip modeled by a repulsive potential, as described by Kelchner et al⁵¹ and the indenter repels all atoms that touch it so that the exerted force has a magnitude of:

$$F_r = -K(r-R)^2 \quad (1)$$

Where K is a force constant, here set to $10\text{eV}/\text{\AA}^3$, r is the distance from the atom to the center of the indenter and R is the radius of the indenter. The force is set to 0 for $r > R$. The indenter radius was set to 10 nm.

Indentation was performed in displacement-controlled mode, similar to other MD studies⁵², using a penetration rate of 5 m/s. Penetration was restricted to a depth in the range of 5 to 7.5 nm for a total simulation time of 1500 ps and a 1 fs timestep. Upon contact with the graphene flake, the reaction force between the flake and the indenter was computed every 0.1 ps to extract load-penetration curves. Indentation was performed at 300K.

Literature review shows that for the derivation of the elastic modulus based on nanoindentation load-displacement curves, the graphene membrane is modeled following the non-linear Föppl membrane theory⁵³. Lee et al⁷ produced a fitting function for the treatment of nanoindentation load-displacement curves in agreement with the non-linear Föppl membrane theory. Namely:

$$F(\delta) = \pi \sigma_0^{2D} \delta + q^3/a^2 E_{2D} \delta^3 \quad (2)$$

Where δ is the deflection, σ_0^{2D} is the membrane pretension, E_{2D} is the two-dimensional Young's modulus, a is the radius of the membrane and q is a correction factor for a Poisson's ratio (ν) other than one third and it takes the form of $q \sim 1.0491 - 0.1462\nu - 0.15827\nu^2$. See Komaragiri et al⁵⁴ for details on the determination of the q function. It can be seen that the linear term of the equation captures the effect of the pre-tension while the cubic term accounts for the effect of the bending stiffness. By using least-square fitting of equation 2 to the load-displacement curves, σ_0^{2D} and E_{2D} can be determined. A discussion about the E2D values obtained compared to experimental values is included in the supplementary material (ESI S1†).

RESULTS AND DISCUSSION

Figure 1a shows the values of the roughness of the membrane as a function of the applied strain before irradiation. Starting from the roughness value of the sample with no strain (0%) we can observe that when a tensile strain is applied, roughness decreases reaching almost a steady value after a strain of about 0.1%. When a compressive strain is applied roughness keeps increasing with increasing compression and the dependence is highly non-linear.

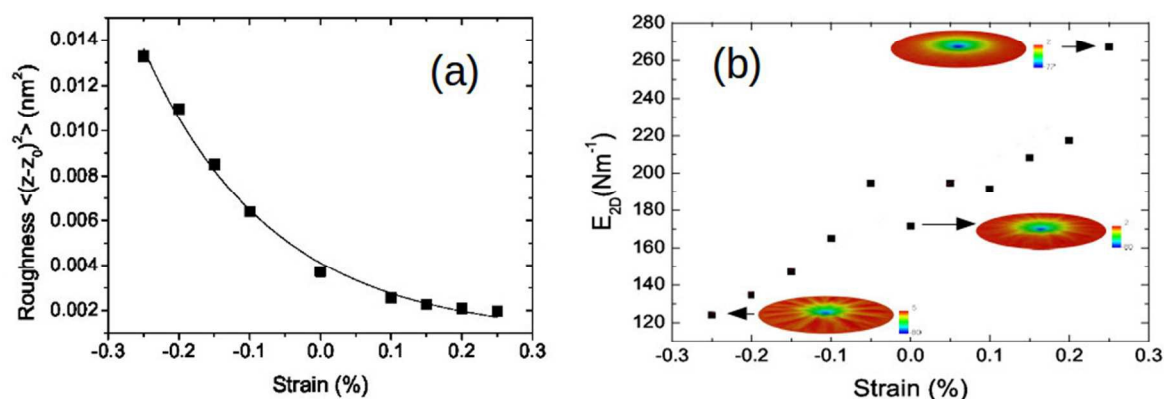


Figure 1: (a) Roughness of the graphene membrane as a function of applied strain before irradiation and (b) E_{2D} obtained from nanoindentation simulations as a function of applied strain. Insets show snapshots of the simulations with colors representing the out-of-plane displacement (in Å).

Nanoindentation simulations have been performed to obtain the E_{2D} and sigma constants for different strains, following the procedure explained above. These two parameters are obtained from a fit to the curves of load as a function of displacement. For an example of these curves see figure S1 in the supplementary material (ESI Fig. S1†). Figure 1(b) shows the values of E_{2D} before irradiation as a function of the applied strain. Clearly strain plays an important role in the mechanical properties of graphene membranes. Compressive strain results in softening of the graphene membrane decreasing the value of the 2D Young's modulus while under tension graphene becomes stiffer. This is in agreement with the results of Lee et al⁴¹ that showed that the presence of ripples results in the softening of graphene since two mechanisms take place: first ripples are smoothed, then, the C-C bond is stretched.

Roughness, as defined above, provides an average value of the fluctuations on the surface, but it is also interesting to see the distribution of these fluctuations. Figure 2 shows a snapshot of the graphene membranes where the colors represent the value of the out-of-plane coordinate of each atom (Z coordinate). Three representative examples are given: figure 2(a) corresponds to a compressive strain of -0.25% , figure 2(b) to a non-strained sample, and figure 2(c) to a tensile strain of 0.25% . Note that the scale changes for each one of the figures.

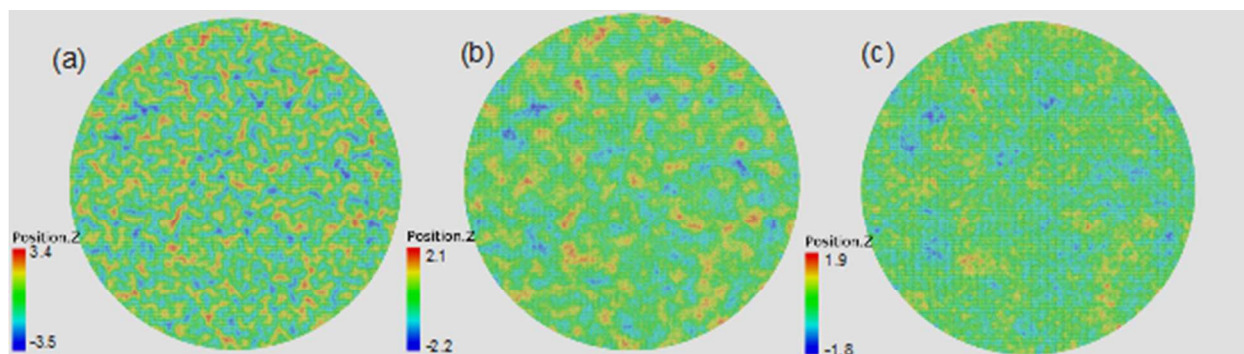


Figure 2: Values of the Z coordinate (in Angstroms) for a graphene membrane and different applied strains before irradiation (a) compressive -0.25% (b) no strain and (c) tensile $+0.25\%$.

This representation allows us to observe the wavelength of these ripples and the effect of strain on their distribution. The wavelength of the ripples decreases under compressive strain, showing a smaller distance between maxima and minima of the ripples in the membrane (see figure 2(a) compared to 2(b), compressed and un-strained respectively). The values of the maximum and minimum increase with respect to those from the sample without strain, with absolute values of about 3.5 \AA for a compressive strain of -0.25% , and of about 2 \AA for the unstrained sample. When a tensile strain is applied the wavelength increases significantly, with maxima and minima farther away from each other, as can be observed in figure 2(c). Also, the values of these maxima and minima decrease, with absolute values of about 1.9 \AA for a 0.25% tensile strain. These changes, however, are much smaller than for a compressive strain, as already shown in figure 1. Observed ripples in our calculations are similar to reported ripples in free-standing graphene measured experimentally⁵⁵.

After relaxation, the sample is irradiated with 140 eV Ar^+ ions following the procedure described in the methods section. Irradiation produces vacancies which are mostly isolated, as well as divacancies and some higher order clusters in much lower concentrations. The efficiency of defect production is about 80% , that is 80 vacancies are created every 100 ions. This is in good agreement with experimental measurements of López-Polín et al³⁷. For the doses studied here (highest dose of $7.5 \times 10^{12} \text{ ions/cm}^2$) the number of vacancies increases linearly with dose, which indicates that the dose is low enough not to have overlap of cascades. The total number of monovacancies is very similar for all strains and doses. However the number of divacancies is slightly higher when samples are under compressive strain and the efficiency of production of divacancies increases with dose (for more information see ESI figure S2†).

Changes in roughness with irradiation dose are presented in Figure 3(a) for two applied strains, a compression of -0.2% and a tension of 0.2% . Differences in roughness induced by the irradiation are quite remarkable. While there are almost no changes when the sample is under a

tensile strain, roughness increases significantly with dose under a compressive strain. Note that changes in roughness induced by the irradiation are over two orders of magnitude larger than those before irradiation for any given strain (see figure 1(a)). Figure 3(b) includes the results of the E2D for the case of two compressive strains (-0.25%, -0.1%), the sample without any initial strain, and two tensile strains (0.1% and 0.25%). Interestingly, the dependence of the Young's modulus with dose follows that of the roughness for the different strains: under tensile strain there is almost no change of the Young's modulus with dose while under compression the Young's modulus increases with dose, at very low doses the E2D does not change significantly but then it becomes stiffer with dose very rapidly. When no strain is applied, there are almost no changes of the E2D with dose.

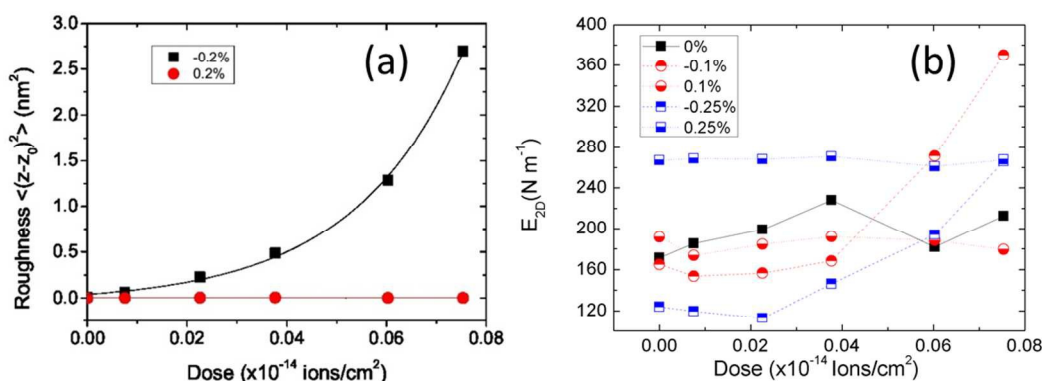


Figure 3: (a) Roughness as a function of dose for two different strains: -0.2% (compressive) and 0.2% (tensile) and (b) values of E2D as a function of dose for different applied strains: compressive -0.25%, -0.1%, (squares, half filled) 0% (squares-filled) and tensile, +0.1% and +0.25% (circles).

Note that the dependence of the E2D shown in figure 3(b) cannot be explained by the production of defects during the irradiation alone since the number of defects increases linearly with dose for all strains applied or for the sample without strain. If defects are the ones responsible for changes in the elastic modulus, the same dependence should be obtained independently of the strain applied, which is not the case here. However, the changes in the elasticity of the graphene membrane follow the dependence shown in figure 3 (a) for the variation of the roughness with dose: when a tensile strain is applied there are no changes in the roughness of the membrane, which results in an almost constant value of the elastic properties, when a compressive strain is considered, the roughness increases with dose with a non-linear dependence just like the elastic Young's modulus.

It is also interesting to point out that under irradiation compressed samples result in stiffer membranes while samples under tension do not present significant differences in the elastic properties. This result seems to contradict those presented in figure 1 for a non-irradiated sample: compressed samples are softer than tensile ones. In order to clarify how radiation influences out-of-plane deformations in the membrane, we present in Figure 4 the Z-coordinates after irradiation for the highest dose simulated: 7.5×10^{12} ions/cm². Figure 4 (a) corresponds to a compressive strain of -0.25%, figure 4 (b) to a non-strained sample and figure 4 (c) to a tensile strain of 0.25%, that is, the same conditions of figure 2 but after irradiation. It is clear from these

figures that the changes induced by irradiation on the out-of-plane deformation are significantly different from those induced only by strain. For the unstrained and compressed samples, irradiation produces a deep well in the membrane, mostly in the center of the sample, removing the ripple distribution existing initially, while under tension a ripple distribution can still be observed in the sample, although the center of the membrane still presents lower valleys than before irradiation. While the sample is almost unaffected when there is an applied tensile strain of about 0.1% or higher, for lower strains or compressive strains the out-of-plane deformations increase. This deformation is not symmetric: the maximum values of Z-coordinate follow the same dependence as observed without irradiation while the minimum values of the Z-coordinate are highly modified by the irradiation. For example, for a -0.25% compression after irradiation, the maximum value of the Z-coordinate is 9 Å while the minimum value is -38 Å. The initial value of the maximum Z-coordinate before irradiation for this same strain is ~ 3.5 Å as shown in figure 2 (a). For the case of the tensile strain of 0.25% the initial maximum value of the Z-coordinate before irradiation is ~ 1.9 Å, which after irradiation changes only slightly to a value of -2.5 Å for the minimum Z-coordinate.

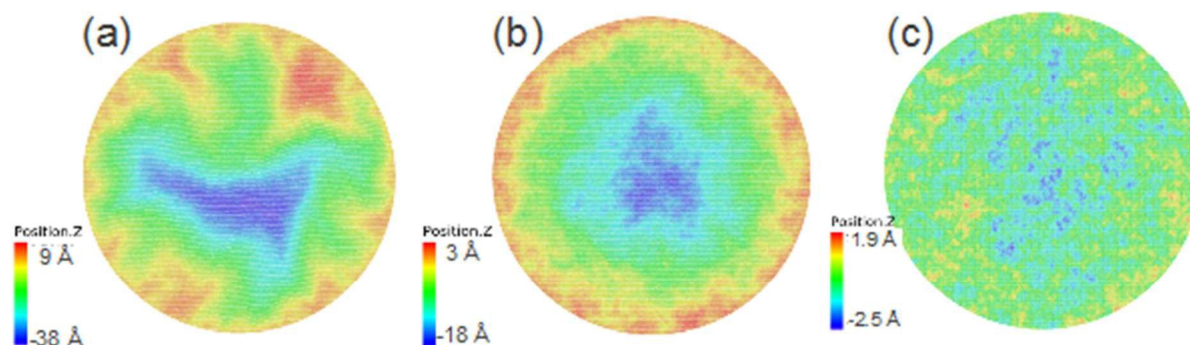


Figure 4: Values of the Z-coordinate (in Å) after 1000 ions or a dose of 7.5×10^{12} ions/cm² for a graphene membrane and different applied strains (a) compressive -0.25% (b) no strain and (c) tensile +0.25%.

These results show that the changes produced by the irradiation with respect to the out-of-plane deformation are very different from those induced by strain but they depend significantly on the initial strain state of the membrane. In the same way that a rippled piece of paper can be flattened covering a larger area, the forward momentum of the energetic particles tends to remove the ripple distribution bowing down the sample and producing a deep valley due to the constrained boundaries. Since compressed samples have more ripples available to be flattened by the energetic particles, this effect is particularly efficient in compressed samples. As a result, the topology of the compressed samples after irradiation approaches that of a tensioned sample, provided the curvature of the valley is neglected as a first approximation, and producing a stiffer response of the sample when subjected to nanoindentation.

These results provide an alternative explanation of recent experimental measurements of the E2D under irradiation³⁷. These experiments show that at very low doses, such as those studied here, there is a strong increase in the E2D, which has been interpreted as the result of defect production. According to López-Polín et al³⁷ vacancies produced by the irradiation quench long range fluctuations resulting in a stiffer membrane. More recent molecular dynamics

simulations³⁴ have attributed the increase in stiffness to the production of monovacancies. In those simulations, however, vacancies are introduced randomly in the sample instead of being the result of an irradiation and no discussion is included with respect to the temperature of the simulations or out-of-plane displacements. Here, we give another interpretation of the effect of irradiation on the elastic properties of a membrane: changes in roughness induced by the irradiation (and not just defect production) are responsible for the changes in mechanical properties.

CONCLUSIONS

Molecular dynamics simulations of graphene membranes irradiated with 140 eV Ar ions with different initial strains, from -0.25% (compression) to 0.25% (tension) have been performed. Defect production rate under these conditions is of about 80% for any of the strains studied, with a slightly higher probability of formation of divacancies when applying a compressive strain than a tensile strain. The concentration of defects increases linearly with dose for all cases studied. Ripples, existing in a free standing graphene, are strongly modified when the membrane is irradiated, and these changes depend on the initial strain applied to the membrane. While the size of these ripples does not change with dose when a tensile strain is applied, under compression there is a non-linear dependence with dose: initially, it only changes slightly and then the roughness increases significantly at higher doses. Moreover, these changes in the ripple distribution induced by the irradiation are different from those induced by strain. Strain gives rise, under compression, to larger ripples with shorter wavelength, while tension results in the opposite behavior, smaller ripples and longer wavelengths. As a result, unirradiated samples under compression are softer than without an applied strain, while samples under tension are stiffer. After irradiation the behavior is quite different: compressed samples are stiffer while samples under tension do not show changes in their mechanical properties. We attribute this difference to the changes in out-of-plane displacements induced by the irradiation which flattens these ripples producing a well that is deeper when the membrane is under compression.

These results provide an alternative way to explain recent experiments of stiffening of graphene membranes under low dose irradiation. Moreover, these simulations point towards paths to tailor the mechanical properties of graphene through a combination of applied strain and irradiation.

Author contributions

J. M-A and C. R. contributed equally to this work. They performed the molecular dynamics simulations and analysis, J. M-A focused on the irradiation calculations and C. R. on the nanoindentation. M. J. C. wrote the first draft of the manuscript, and all authors contributed to the writing, analysis and discussion.

ACKNOWLEDGEMENTS

We want to thank Professors Cristina Gómez-Navarro, Juan José Palacios and Joaquín Fernandez-Rossier for fruitful discussions. The simulations have been done in the supercomputer MareNostrum at Barcelona Supercomputing Center - Centro Nacional de Supercomputación (The Spanish National Supercomputing Center) as well as in the computers of the Dept. of Applied Physics at the UA. This work is supported by the Generalitat Valenciana through grant reference PROMETEO2012/011 and the Spanish government through grant FIS2010-21883. CJR and EMB thanks support from SeCTyP-UNCuyo grant M003, and ANPCyT grant PICT-2014-0696. CJR thanks CONICET and the 310 Group at FCEN-UNCuyo.

REFERENCES

1. K. Geim and K. S. Novoselov, *Nat. Mater.*, 2007, **6**, 183-191
2. K. S. Novoselov, Z. Jiang, Y. Zhang, S. V. Morozov, H. L. Stormer, U. Zeitler, J. C. Maan, G. S. Boebinger, P. Kim and A. K. Geim, *Science*, 2007, **315**, 1379
3. S. Ghosh, I. Calizo, D. Teweldebrhan, E. P. Pokatilov, D. L. Nika, A. A. Balandin, W. Bao, F. Miao and C. N. Lau, *Appl. Phys. Lett.*, 2008, **92**, 151911
4. J. Hu, X. Ruan and Y. P. Chen, *Nano Lett.*, 2009, **9**, 2730-2735
5. Y. W. Son, M. L. Cohen and S. G. Louie, *Nature*, 2006, **444**, 347-349
6. F. Bonaccorso, Z. Sun, T. Hasan and A. C. Ferrari, *Nature Photonics*, 2010, **4**, 611-622
7. C. Lee, X. Wei, J. W. Kysar and J. Honer, *Science*, 2008, **321**, 385-388
8. L. A. Ponomarenko, F. Schedin, M. I. Katsnelson, R. Yang, E. W. Hill, K. S. Novoselov and A. K. Geim, *Science*, 2008, **320**, 356-358
9. X. Wang, X. Li, L. Zhang, Y. Yoon, P. K. Weber, H. Wang, J. Guo and H. Dai, *Science*, 2009, **324**, 768-771
10. Y. -M. Lin, C. Dimitrakopoulos, K. A. Jenkins, D. B. Farmer, H. -Y. Chiu, A. Grill and Ph. Avouris, *Science*, 2010, **327**, 662
11. S. Bae, H. Kim, Y. Lee, X. Xu, J. -S. Park, Y. Zheng, J. Balakrishnan, T. Lei, H. Kim, Y. Song, Y. -J. Kim, K. S. Kim, B. Özyilmaz, J. -H. Ahn, B. Hong and S. Iijima, *Nature Nanotechnology*, 2010, **5**, 574-578
12. K. S. Novoselov, Novoselov, A. K. Geim, S. V. Morozov, D. Jiang, Y. Zhang, S. V. Dubonos, I. V. Grigorieva and A. A. Firsov, *Science*, 2004, **306**, 666-669
13. S. M. Chowdhury, G. Lalwani, K. Zhang, J. Y. Yang, K. Neville and B. Sitharaman, *Biomaterials*, 2013, **34**, 283-293
14. Q. He, H. G. Sudibya, Z. Yin, S. Wu, H. Li, F. Boey, W. Huang, P. Chen and H. Zhang, *ACS Nano*, 2010, **4**, 3201-3208
15. F. Torrisi, T. Hasan, W. Wu, Z. Sun, A. Lombardo, T. S. Kulmala, G. -W. Hsieh, S. Jung, F. Bonaccorso, P. J. Paul, D. Chu and A. C. Ferrari, *ACS Nano*, 2012, **6**, 2992-3006
16. Industrial & Specialty Printing, http://industrial-printing.net/content/developments-conductive-inks#_Vp5vNJrhBdg (accessed January 2016)
17. A. Hashimoto, K. Suenaga, A. Gloter, K. Urita and S. Iijima, *Nature*, 2004, **430**, 870-873
18. M. M. Ugeda, I. Brihuega, F. Guinea and J. M. Gómez-Rodríguez, *Phys. Rev. Lett.*, 2010, **104**, 096804
19. H.-M. Chien, M.-C. Chuang, H. -C. Tsai, H. -W. Shiu, L. -Y. Chang and C. -H. Chen, *Carbon*, 2014, **80**, 318-324
20. J. Martinez-Asencio and M. J. Caturla, *Nuclear Instruments and Methods in Physics Research Section B: Beam Interactions with Materials and Atoms*, 2015, **352**, 225-228
21. W. Li, L. Liang, S. Zhao, S. Zhang and J. Xue, *J. Appl. Phys.*, 2013, **114**, 234304
22. C. Jin, F. Lin, K. Suenaga and S. Iijima, *Phys. Rev. Lett.*, 2009, **102**, 195505
23. S. Zhao, J. Xue, Y. Wang, S. Yan, Effect of SiO₂ substrate on the irradiation-assisted manipulation of supported graphene: a molecular dynamics study, *Nanotechnology* 2012, **23**, 285703
24. W Li, X Wang, X Zhang, S Zhao, H Duan, J Xue, Mechanism of the defect formation in supported graphene by energetic heavy ion irradiation: the substrate effect, *Sci Rep.* 2015, **5**, 9935
25. Q. Wang, Y. Shao, D. Ge, Q. Yang and N. Ren, Surface modification of multilayer graphene using Ga ion irradiation, *J. Appl. Phys.* 2015, **117**, 165303
26. K. Liu , C.-L. Hsin , D. Fu , J. Suh , S. Tongay , M. Chen , Y. Sun , A. Yan , J. Park , K. M. Yu , W. Guo , A. Zettl, H. Zheng , D. C. Chrzan , J. Wu, Self-Passivation of Defects:

Effects of High-Energy Particle Irradiation on the Elastic Modulus of Multilayer Graphene, *Adv. Mater.* 2015, **27**, 6841–6847

27. Y. Asayama, M. Yasuda, K. Tada, H. Kawata and Y. Hirai, *Vac. Sci. Technol. B*, 2012, **30**, 06FJ02
28. P. Bellido and J. M. Seminario, *J. Phys. Chem. C*, 2012, **116**, 4044-4049
29. X. -M. Qin, T. -H. Gao, W. -J. Yan, X. -T. Guo and Q. Xie, *J. Phys. Chem. C*, 2012, **1061**, 19-25
30. O. Lehtinen, J. Kotakoski, A. V. Krasheninnikov, A. Tolvanen, K. Nordlund and J. Keinonen, *Phys. Rev. B*, 2010, **81**, 153401
31. J. Kotakoski, C. H. Jin, O. Lehtinen, K. Suenaga and A. V. Krasheninnikov, *Phys. Rev. B*, 2010, **82**, 113404
32. J. Kotakoski, C. Brand, Y. Lilach, O. Cheshnovsky, C. Mangler, M. Arndt and J. C. Meyer, *Nano Lett.*, in press
33. H. Åhlgren, S. K. Hämäläinen, O. Lehtinen, P. Liljeroth and J. Kotakoski, *Phys. Rev. B*, 2013, **88**, 155419
34. L. Tapasztó, G. Dobrik, P. Nemes-Incze, G. Vertesy, Ph. Lambin and L. P. Biró, *Phys. Rev. Lett.*, 2008, **78**, 233407
35. C. Gómez-Navarro, M. Burghard and K. Kern, *Nano Lett.*, 2008, **8**, 2045-2049
36. G. -H. Lee, R. C. Cooper, S. J. An, S. Lee, A. van der Zande, N. Petrone, A. G. Hammemburg, C. Lee, B. Crawford, W. Oliver, J. W. Kysar and J. Hone, *Science*, 2013, **340**, 1073-1076
37. G. López-Polín, C. Gómez-Navarro, V. Parente, F. Guinea, M. I. Katsnelson, F. Pérez-Murano and J. Gómez-Herrero, *Nature Physics*, 2014, **11**, 26-31
38. D. G. Kvashnin and P. B. Sorokin, *The Journal of Physical Chemistry Letters*, 2015, **6**, 2384
39. A. Fasolino, J. H. Los and M. I. Katsnelson, *Nat. Mat.*, 2007, **6**, 858
40. J. C. Meyes, A. K. Geim, M. I. Katsnelson, T. J. Booth and S. Roth, *Nature*, 2007, **446**, 60
41. S. Lee, *Nanoscale Research Letters*, 2015, **10**, 422
42. D. Yoon, Y. -W. Son and H. Cheong, *Nano Lett.*, 2011, **11**, 3227
43. G. Gui, Z. Jianxin and M. Zhenqiang, *J. Phys. Conf. Ser.*, 2012, **402**, 012004
44. W. Bao, F. Miao, Z. Chen, H. Zhang, W. Jang, C. Dames and C. N. Lau, *Nat. Nano*, 2009, **4**, 562
45. S. Plimpton, *J. Comp. Phys.*, 1995, **117**, 1-19
46. J. Tersoff, *Phys. Rev. Lett.*, 1988, **61**, 2879
47. F. Ziegler, J. P. Biersack and U. Littmark, *The Stopping and Range of Ions in Solids*, Pergamon Press, New York, 1985
48. N. Inui, K. Mochiji and K. Moritani, *Nanotechnology*, 2008, **19**, 505501
49. E. Polak and G. Ribière, *Revue Française d'Informatique et de Recherche Opérationnelle*, 1969, **16**, 35-43
50. A. Stukowski, *Modelling Simul. Mater. Sci. Eng.*, 2010, **18**, 015012
51. L. Kelchner, S. Plimpton and J. C. Hamilton, *Phys. Rev. B*, 1998, **58**, 11085
52. W. Jiang, J. -S. Wang and B. Li, *Phys. Rev. B*, 2009, **80**, 113405
53. A. Libai, A., and Simmonds, J. G., 1998, *The Non-Linear Theory of Elastic Shells*, 2nd ed., Cambridge University Press, Cambridge
54. U. Komaragiri, M. R. Begley and J. G. Simmonds, *J. Appl. Mech.*, 2005, **72**, 203
55. U. Monteverde, J. Pal, M.A. Migliorato, M. Missous, U. Bangert, R. Zan, R. Kashtiban, D. Powell, Under pressure: Control of strain, phonons and bandgap opening in rippled graphene, *Carbon* 2015, **91**, 266-274